Title

Quantification of DNA Lesions Induced by 4-(Methylnitrosamino)-1-(3-pyridyl)-1-butanol in Mammalian Cells.

Journal

Chemical Research in Toxicology, 32(4)

Authors

Guo, Su
Leng, Jiapeng
Tan, Ying
et al.

Publication Date

2019-04-15

DOI

10.1021/acs.chemrestox.8b00374

Peer reviewed

HHS Public Access

Author manuscript

Chem Res Toxicol. Author manuscript; available in PMC 2020 April 15.

Published in final edited form as:

Chem Res Toxicol. 2019 April 15; 32(4): 708–717. doi:10.1021/acs.chemrestox.8b00374.

Quantification of DNA Lesions Induced by 4–(Methylnitrosamino)-1-(3-pyridyl)-1-butanol in Mammalian Cells

Su Guo[†], **Jiapeng Leng**[‡], **Ying Tan**[†], **Nathan E. Price**[‡], and **Yinsheng Wang**[*,†,‡]

[†]Environmental Toxicology Graduate Program, University of California, Riverside, California 92521-0403, United States

[‡]Department of Chemistry, University of California, Riverside, California 92521-0403, United States

Abstract

Quantitative measurement of DNA adducts in carcinogen-exposed cells provides the information about the frequency of formation and the rate of removal of DNA lesions *in vivo*, which yields insights into the initial events of mutagenesis. Metabolic activation of tobacco-specific nitrosamines, 4-(methylnitrosamino)-1-(3-pyridyl)-1-butanone (NNK) and its reduction product 4-(methylnitrosamino)-1-(3-pyridyl)-1-butanol (NNAL), leads to pyridyloxobutylation and pyridylhydroxybutylation of DNA. In this study, we employed a highly robust nanoflow liquid chromatography-nanoelectrospray ionization-tandem mass spectrometry (nLC-nESI-MS/MS) coupled with the isotope-dilution method for simultaneous quantification of O^6-[4-(3-pyridyl)-4-hydroxylbut-1-yl]-2′-deoxyguanosine (O^6-PHBdG) and O^2- and O^4-[4-(3-pyridyl)-4-hydroxylbut-1-yl]-thymidine (O^2-PHBdT and O^4-PHBdT). Cultured mammalian cells were exposed to a model pyridylhydroxybutylating agent, 4-(acetoxymethylnitrosamino)-1-(3-pyridyl)-1-butanol (NNALOAc), followed by DNA extraction, enzymatic digestion, and sample enrichment prior to nLC-nESI-MS/MS quantification. Our results demonstrate, for the first time, that O^4-PHBdT is quantifiable in cellular DNA and naked DNA upon NNALOAc exposure. We also show that nucleotide excision repair (NER) machinery may counteract the formation of O^2-PHBdT and O^4-PHBdT, and O^6-alkylguanine DNA alkyltransferase (AGT) may be responsible for the repair of O^6-PHBdG and O^4-PHBdT in mammalian cells. Together, our study provides new knowledge about the occurrence and repair of NNAL-induced DNA lesions in mammalian cells.

Graphical Abstract

[*]**Corresponding Author:** Tel.: (951) 827-2700. Fax: (951) 827-4713. Yinsheng.Wang@ucr.edu.

ASSOCIATED CONTENT

Supporting Information

The Supporting Information is available free of charge on the ACS Publications website at DOI: 10.1021/acs.chemrestox.8b00374. Figures S1−S3 (ESI-MS and MS/MS of O^4-PHBdT, O^2-PHBdT, and O^6-PHBdG and their stable isotope-labeled derivatives); Figure S4 (HPLC trace for the enrichment of O^4-PHBdT, O^2-PHBdT, and O^6-PHBdG from the enzymatic digested monomers of genomic DNA isolated from NNALOAc-treated cells); Figure S5 (calibration curves for the quantifications of O^4-PHBdT, O^2-PHBdT, and O^6-PHBdG). Table S1 (accurate mass measurement results for the $[M + H]^+$ ions of unlabeled and the stable isotope-labeled O^4-PHBdT, O^2-PHBdT, and O^6-PHBdG) (PDF)

Notes

The authors declare no competing financial interest.

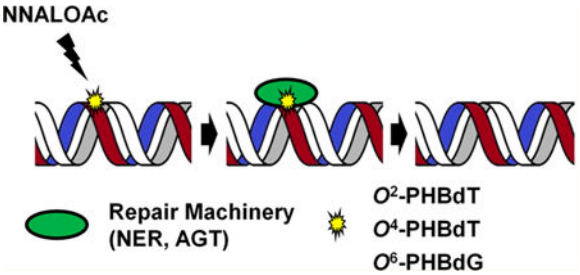

INTRODUCTION

The human genome is susceptible to damage by endogenous metabolites and exogenous chemicals.[1,2] The resulting DNA damage leads to perturbations of genomic stability, which may give rise to mutagenesis and other adverse biological consequences.[3] Tobacco-specific nitrosamines may contribute to human cancer, and they are associated with the elevated lung cancer rate in the cohorts of active tobacco users in several epidemiological studies.[4–6] 4-(Methylnitrosamino)-1-(3-pyridyl)-1-butanone (NNK), a major tobacco-specific nitrosamine, and its reduced metabolite 4-(methylnitrosamino)-1-(3-pyridyl)-1-butanol (NNAL) have been found to induce cancer in rodents in pioneering studies by Hecht and co-workers.[7–9] Carcinogenesis from exposure to NNK and NNAL arises after they give rise to adducts on the nucleobases and backbone of DNA, which in turn results in compromised DNA replication and leads to mutations in DNA.[10,11]

Some earlier studies by Hecht and others demonstrated that a subset of cytochrome P450 enzymes participate in activation of NNK and NNAL,[11–14] which as a result gives rise to reactive intermediates that can pyridyloxobutylate and pyridylhydroxybutylate DNA, respectively (Scheme 1). A number of studies showed the presence of DNA lesions in mammalian genome due to pyridyloxobutylation and pyridylhydroxybutylation. These lesions include O^2 -POBdT,[15–17] O^4 -POBdT,[18] O^6 -POBdG,[15,17,19] O^2-PHBdT,[15] O^6-PHBdG,[15,17] O^2-POBdC,[17] 7-POBG,[15,17] 7-PHBG,[15] N^6-POBdA,[20] N^6-PHBdA,[20] $N1$-POBdI,[20] and $N1$-PHBdI[20] on nucleobases and B_1p(POB)-B_2[21–23] and B_1p(PHB)B_2[21–23] on phosphate backbone. Most lesions mentioned above exhibited cytotoxic and mutagenic properties, which, if not properly repaired, may impede the transmission of genetic information by disrupting DNA replication and transcription machineries. Du et al.[24] demonstrated recently that O^2-POBdT and O^4-POBdT could moderately block DNA replication, which elicited T → A transversion and T → C transition, respectively, whereas G → A transition constituted the major form of mutation induced by O^6-POBdG. The activated form of NNK and NNAL may also serve as a potent methylating agent. The resulting level of O^6-methylguanine (O^6-mG) following NNK exposure was found to be correlated with tumorgenicity.[19,25] Ma et al.[26] also demonstrated recently that B_1pmeB_2 can be induced *in vivo* upon exposure to NNK and NNAL.

Mammalian cells contain a complex arsenal of DNA repair proteins to remove deleterious DNA lesions.[1,2,27] In this vein, various classes of mammalian DNA repair proteins are capable of removing pyridyloxobutylated and pyridylhydroxybutylated DNA-modifications. O^6-alkylguanine-DNA alkyltransferase (AGT) was found capable of removing directly the

POB remnant from O^6-POBdG.[17,19,28] There are also studies revealing that O^2-POBdT contributes to the elevated occurrence of AT → TA mutation in cells deficient in nucleotide excision repair (NER); therefore, NER is likely an important pathway for the repair of this lesion.[28]

Although the implications of tobacco-specific nitrosamines in carcinogenesis have been well documented,[14,29,30] there are still gaps to be filled in establishing reliable quantification methods to meet the increasing demands for assessing the risk of tobacco consumption. In this respect, methods including ^{32}P-postlabeling assay, excision assay, and immunoblot analysis have been used for measuring the levels and assessing the repair of targeted DNA lesions *in vitro* and *in vivo*.[31,32] Due to its high sensitivity and its capacity in providing structural information,[18,33–41] mass spectrometry has become a tool of choice in DNA adduct analysis. In this vein, solid-phase extraction followed by LC-MS/MS analysis was previously used for quantifying several pyridyloxobutyl and pyridylhydroxybutyl DNA lesions.[17,21,23,26,28]

Herein, we report the application of a highly sensitive nanoflow liquid chromatography-nanoelectrospray ionization tandem mass spectrometry (nLC-nESI-MS/MS) coupled with the stable isotope-dilution technique for the simultaneous quantifications of O^4-PHBdT, O^2-PHBdT, and O^6-PHBdG. This is the first reported measurement of O^4-PHBdT in mammalian cells (Scheme 1). By employing this method, we further explored how the three lesions are repaired in cultured mammalian cells.

EXPERIMENTAL SECTION

Materials.

Unless further specified, all chemicals were obtained from Sigma-Aldrich (St. Louis, MO), and enzymes were obtained from New England Biolabs (Ipswich, WA). NNALOAc was obtained by the reduction of NNKOAc (Toronto Research Chemicals Inc., North York, Ontario) using $NaBH_4$. The reaction was carried out under a condition where NNKOAc (10 mg) was mixed with 5 equiv of $NaBH_4$ in methanol at room temperature for 30 min, and the product NNALOAc was then isolated from the reaction mixture using HPLC. *Erythro*-9-(2-hydroxy-3-nonyl)adenine (EHNA) hydrochloride was obtained from Tocris Bioscience (Ellisville, MO). Repair-competent and ERCC1-deficient AA8 Chinese hamster ovary (CHO and ERCC1, CHO-7−27)[42] cells were provided by M. M. Seidman (National Institute of Aging, Bethesda, MD). Human skin fibroblasts with repair proficiency (GM00637) and deficiency in xeroderma pigmentosum (XPA, GM04429) were kind gifts from G. P. Pfeifer (Van Andel Research Institute, Grand Rapids, MI).

Preparation of Standards.

O^2-PHBdT, O^6-PHBdG, O^4-PHBdT, and the respective stable isotope-labeled derivatives were obtained by reduction with $NaBH_4$ of previously synthesized O^2-POBdT, O^6-POBdG, and O^4-POBdT.[18] Unlabeled and stable isotope-labeled O^4-PHBdT have not been previously synthesized and were made specifically for this study. The reaction was carried out by mixing O^4-POBdT (100 μg) with 5 equiv of $NaBH_4$ in 100 μL methanol at room

temperature for 10 min. The solution was diluted with 9 volumes of water, and the mixture was subjected to extraction with an equal volume of ethyl acetate for three times. The aqueous layer was collected, and the overall yield was 80%. Exact mass measurements (Thermo Q-Exactive Plus) yielded m/z 392.1820 and 396.2076 for the $[M + H]^+$ ions of the O^4-PHBdT and [pyridine-d_4]-O^4-PHBdT, respectively, which are in agreement with their respective calculated m/z values of 392.1822 and 396.2073 (Table S1, Figure S1). O^2-PHBdT and O^6-PHBdG were prepared following similar procedures and characterized similarly (Table S1, Figures S2−S3).

Treatment of Calf Thymus DNA with NNALOAc and Porcine Liver Esterase.

Calf thymus DNA (25 μg) was treated with 10 or 50 μg NNALOAc and porcine liver esterase (0.4 U) in 0.1 M phosphate buffer (1 mL, pH 7.0) at 37 °C overnight. The resulting mixture was first extracted with an equal-volume mixture of $CHCl_3$/isoamyl alcohol (24:1, v/v), followed by ethyl acetate extraction. The DNA was precipitated from the aqueous phase by adding cold ethanol, washed sequentially with 70% ethanol and then with 100% ethanol, allowed to air-dry at room temperature, redissolved in doubly distilled water, and kept at−20 °C until enzymatic digestion and subsequent LC-MS/MS analysis.

Cell Culture and Treatment with NNALOAc.

All cells were cultured at 37 °C in a 5% CO_2 atmosphere with media containing 10% fetal bovine serum and 100 IU/mL penicillin: Human skin fibroblasts were grown in Dulbecco's modified Eagle's medium (Gibco), and CHO cells were grown in Alpha Minimum Essential Medium (Gibco) without ribonucleosides or 2′-deoxyribonucleosides. Cells were seeded (approximately $1-1.5 \times 10^6$) in 75 cm^2 flasks and cultured for 24 h. The cells were unexposed or exposed with 5, 10, or 25 μM of NNALOAc. The GM00637 human skin fibroblast cells were treated with 10 μM NNALOAc alone or concurrently with 20 μM O^6-benzylguanine, an AGT inhibitor. After a 24 h treatment, the medium was removed from the flask, and the cells were washed twice with phosphate-buffered saline (1 × PBS) to remove any remaining NNALOAc. During repair studies, cells were maintained at 37 °C in their respective fresh media, detached using trypsin-EDTA at different time intervals and centrifuged into a cell pellet.

DNA Extraction and Enzymatic Digestion.

Standard procedures for DNA extraction, enzymatic digestion, and HPLC enrichment were utilized for the targeted pyridylhydroxybutylated nucleosides and are detailed previously.[18,36,38] A representative chromatogram for off-line HPLC enrichment is shown in Figure S4, and the detailed procedures are provided in the Supporting Information.

nLC-nESI-MS/MS Analysis.

Online nLC-nESI-MS/MS measurements were conducted on a TSQ-Vantage triple quadrupole mass spectrometer (Thermo Fisher Scientific, CA) equipped with a nanoelectrospray ionization source and coupled with an EASY nLC II system (Thermo Fisher Scientific, CA). HPLC separation was conducted by employing a trapping column (150 μm × 40 mm) and an analytical column (75 μm × 200 mm), both packed in-house with

Magic C18 AQ (200 Å, 5 μm, Michrom BioResource, Auburn, CA). Mobile phases A and B were 0.1% formic acid in doubly distilled H_2O and acetonitrile, respectively. Initially, the sample was loaded, at a flow rate of 3 μL/min for 5 min, onto the trapping column with mobile phase A. The modified nucleosides were eluted through a 40 min linear gradient of 0−50% mobile phase B with a flow rate of 300 nL/min. The TSQ-Vantage mass spectrometer was operated in the selected-reaction monitoring (SRM) mode. We monitored the transitions corresponding to the neutral loss of a deoxyribose (116 Da) from the $[M + H]^+$ ions of the three modified nucleosides (i.e., m/z 392 → 276, 392 → 276, and 417 → 301 for O^2-PHBdT, O^4-PHBdT, and O^6-PHBdG, respectively) and their stable isotope-labeled counterparts (i.e., m/z 396 → 280, 396 → 280, and 421 → 305, Figure 1). The voltage for electrospray was set at 2.0 kV, and the ion transfer tube was heated to 275 °C. The widths for precursor ion and product ion isolation were 3 and 0.7 Da, respectively, with a dwell time for 1.25 s. The collision gas was 1.2 mTorr argon, and the collision energy was 15 V. The limit of quantitation (LOQ) here is defined as the amount of analyte needed to yield a signal that is the sum of the mean signal and 10 times the standard deviation of signal from three blank runs in the selected-ion chromatograms (SICs) plotted for the transitions used for analyte quantification.

METHOD DEVELOPMENT

The intra- and interday precision and accuracy of the O^2-PHBdT, O^4-PHBdT, and O^6-PHBdG measurements were gathered from three different concentrations of each analyte. The samples used for calibration curve generation or precision and accuracy test were comprised of 5 μg calf thymus DNA mixed with standard solutions of the three lesion-containing oligodeoxyribonucleotides (ODNs, 5′-ATGGCGXGCTAT-3′, where 'X' represents O^2-PHBdT, O^4-PHBdT, or O^6-PHBdG) and their corresponding stable isotope-labeled mononucleosides. The samples from cellular DNA were prepared following previously described procedures [18,36,38] and were subjected to LC-MS/MS measurements. Calibration curves were obtained from triplicate analyses, and the molar ratios of the unlabeled ODNs to their stable isotope-labeled counterparts were 0.10, 0.50, 1.00, 2.00, 5.00, 10.0, and 20.0 for O^2-PHBdT and O^6-PHBdG, and O^4-PHBdT, with the amount of the labeled nucleosides being 5 fmol each. Calibration curves were constructed using SIC peak area ratios for the unlabeled/labeled standards versus the molar ratios of unlabeled/labeled standards and fitting a straight line (Figure S5). The moles of DNA lesions in the nucleoside mixtures were calculated from the peak area ratios found in the SICs for the analytes and compared to their corresponding stable isotope-labeled counterparts. The final levels of DNA lesions were displayed as number of lesions per 10^8 nucleosides and were calculated by dividing the number of moles of modified by moles of total nucleosides in the digestion mixture.

RESULTS

In this study, we aimed to set up a robust method for the quantification of *O*-pyridylhydroxybutylated dT and dG lesions in enzymatically digested cellular DNA using nLC-nESI-MS/MS coupled with the stable-isotope-dilution, and we set out to employ the method for examining the occurrence and repair of these lesions in mammalian cells.

Syntheses of Unlabeled and Stable Isotope-Labeled Standards.

We prepared the unlabeled and stable isotope-labeled standards for O^2-PHBdT, O^4-PHBdT, and O^6-PHBdG (see Experimental Section). O^4-PHBdT is a novel pyridylhydroxylbutylated DNA lesion that we synthesized through reduction of the previously synthesized O^4-POBdT.[18]

Quantification of O^2-PHBdT, O^4-PHBdT, and O^6-PHBdG Lesion Using nLC-nESI-MS/MS.

We next employed the nLC-nESI-MS/MS method for accurate quantifications of O^2-PHBdT, O^4-PHBdT, and O^6-PHBdG. The LOQs of these three analytes were determined to be 24.0, 19.0, and 8.5 amol, which correspond to 7.4, 5.9, and 2.6 modifications per 10^{10} nucleosides, respectively, when 10 μg DNA is used for analysis. The procedures for sample preparation are described in detail in the Experimental Section, where the cellular samples were subjected to DNA extraction using a high-salt method, RNA removal, and enzymatic digestion with a cocktail of four enzymes, including both 3′ and 5′ exonucleases to release DNA lesions as mononucleosides. The stable isotope-labeled O^2-PHBdT, O^4-PHBdT, and O^6-PHBdG were added prior to DNA digestion, which corrects for the potential analyte loss during the extraction and HPLC enrichment steps. We then evaluated the intra- and interday precision and accuracy by triplicate measurements of calf thymus DNA (10 μg) mixed with various concentrations of lesion-bearing ODNs. Our results demonstrate that the precision (relative standard deviation: 3.8−14.9%) and accuracy (recovery: 84.9−97.1%) for the method were reasonably good (Table 1).

The detection of DNA modifications of low abundance is challenging, where the sensitivity for analyte measurement is sometimes compromised by much larger amounts of canonical nucleosides released from DNA and buffer salts included in the enzymatic digestion reaction. To address this issue, we conducted offline LC enrichment before LC-MS/MS analysis. The LC-MS/MS conditions were optimized prior to sample analysis. Better sensitivity could be obtained in the positive-ion mode, which was used along with 0.1% formic acid (v/v) in the mobile phase to improve protonation of the analytes.

Dose-Dependent Formation of O^2-PHBdT, O^4-PHBdT, and O^6-PHBdG in Mammalian Cells.

After successfully developing a robust method for nLC-nESI-MS/MS analysis, we next employed the method to quantify the levels of O^2-PHBdT, O^4-PHBdT, and O^6-PHBdG in genomic DNA. The DNA samples were isolated from Chinese hamster ovary cells or human skin fibroblasts exposed with varied concentrations of NNALOAc. NNALOAc was used as a cell membrane-permeable precursor to the reactive intermediate in the presence of cellular esterase (Scheme 1). All three modified nucleosides formed in a dose-dependent manner with increasing concentration of NNALOAc (Figure 2). When the concentration of NNALOAc was increased from 5 to 25 μM, the amount of O^4-PHBdT in the XPA-proficient GM00637 cells and XPA-deficient GM04429 cells increased from 5.8 to 33.0 and from 9.5 to 53.1 lesions per 10^8 nucleosides, respectively (Figure 2B). Similar elevated levels of O^4-PHBdT were observed in Chinese hamster ovary cells, where in ERCC1-deficient CHO-7−27 cells and in repair-proficient CHO-AA8 cells, the respective frequencies of O^4-PHBdT were 16.4−71.5 and 12.0−47.4 lesions per 10^8 nucleosides (Figure 2E). Our

quantification data also showed that the levels of O^2-PHBdT and O^6-PHBdG were significantly higher than that of O^4-PHBdT in mammalian cells.

The pronounced difference in occurrence between O^2-PHBdT and its regioisomeric O^4-PHBdT might arise from the differences in their rate of formation or repair. To explore the former possibility, we exposed calf thymus DNA to NNALOAc together with porcine liver esterase and quantified the frequencies of the three lesions using the aforementioned workflow (Figure 3). Our *in vitro* results validated the preferential formation O^2-PHBdT over O^4-PHBdT, while O^6-PHBdG formed at higher levels than either of the other two lesions. The levels of O^2-PHBdT, O^4-PHBdT and O^6-PHBdG—relative to one another—were in line with what were previously reported for the corresponding POB adducts in calf thymus DNA treated with NNKOAc and esterase.[18,22,39]

Removal of O^2-PHBdT, O^4-PHBdT, and O^6-PHBdG in Mammalian Cells.

Our quantification results reveal that the two lines of NER-deficient cells (i.e., XPA-deficient GM04429 and ERCC1-deficient CHO-7−27) exhibited significantly higher levels of O^2-PHBdT and O^4-PHBdT compared to their repair-competent counterparts (GM00637 and CHO-AA8). These results substantiate the notion that NER is involved in removal of these two lesions from cellular DNA. To further assess the involvement of NER in repairing these lesions, we also measured the frequencies of the three pyridylhydroxybutyl lesions in the cells at 0, 12, and 24 h after treatment with 10 μM NNALOAc (Figure 4). No pronounced cell death was observed at the end of NNALOAc exposure. Our results showed that the rates of decrease of this specific lesion were comparable in human skin fibroblasts cells and Chinese hamster ovary cells. In addition, the levels of O^2-PHBdT in NER-proficient and NER-deficient cells were significantly different at all three time points following NNALOAc exposure, substantiating that O^2-PHBdT is a good substrate for NER (Figure 4A,D). To a lesser degree, O^4-PHBdT is also affected by NER, as supported by the quantification data obtained for this lesion in NER-deficient cells and their repair-proficient counterparts (Figure 4B,E). O^6-PHBdG was found not to be an NER substrate, as the levels of this lesion in NER-deficient cells are not significantly different from that in NER-proficient cells measured at all time points (Figure 4C,F). We also observed that the CHO cells and human skin fibroblasts cells exhibited different repair efficiencies for O^6-PHBdG, suggesting that AGT may be involved in repairing this specific lesion, since there is no AGT expression in CHO cells.[17,19,28,43] In this vein, it is of note that the time-dependent decrease in the levels of the three lesions is attributed, in part, to the increase in cell numbers over time.

We also asked whether AGT participated in the removal of the three lesions. Toward this end, we exposed GM00637 cells with 10 μM NNALOAc alone, or in conjunction with 20 μM O^6-benzylguanine, and measured the levels of the three lesions at 24 h after exposure. Along this line, it was observed previously that treatment of cultured mammalian cells with 20 μM O^6-benzylguanine could result in the ubiquitination and proteasomal degradation of AGT protein, where the protein is almost undetectable at 18 h following the treatment.[44] It turned out that the levels of O^2-PHBdT in the control and AGT-depleted cells were almost the same (Figure 5A). We detected a small difference in the levels of O^4-PHBdT in

GM00637 cells with or without O^6-benzylguanine treatment (Figure 5B), indicating that AGT may also be involved in the removal of O^4-PHBdT.[27,45] The difference in O^6-PHBdG levels was the largest among the three lesions (Figure 5C), suggesting that AGT readily repairs this lesion.

DISCUSSION

LC-MS/MS in combination with the stable isotope-dilution method enables specific, accurate, and highly sensitive measurement of DNA lesions in complex biological matrices.[18,33–41] It is advantageous over conventional DNA adduct measurement methods (e.g., immunoblot assay, ^{32}P-postlabeling)[46–48] by offering structural information to enable identification and by facilitating reliable absolute quantification when spiked with known amounts of stable isotope-labeled standards.[40,49,50] In this study, stable isotope-labeled standards were added prior to enzymatic digestion, which helps correct for the loss of analytes during chloroform extraction and offline enrichment; thereby providing more accurate quantification for the three lesions. Additionally, offline HPLC was employed to eliminate the more abundant canonical nucleosides in digestion mixtures and remove buffer salts used during the enzymatic digestion. Our offline HPLC enrichment method provides higher sensitivity in subsequent LC-MS/MS analysis compared to previously reported solid-phase extraction methods for targeted nucleoside enrichment; this lower sensitivity may have been due to incomplete removal of unmodified nucleosides and buffer salts during solid-phase extraction.[51,52] The calibration curve established in this study employed calf thymus DNA spiked with lesion-bearing ODNs, which allowed us to correct for potential incomplete release of modified nucleosides from DNA during the digestion step.

Mammalian cells contain an arsenal of DNA repair proteins that can be dispatched in response to numerous types of damage, thus protecting genomic stability. Here we used four lines of mammalian cells that are proficient or deficient in key NER proteins, and we investigated the role of NER in the removal of O^2-PHBdT, O^4-PHBdT, and O^6-PHBdG from genomic DNA. Dose-dependent formation was observed for O^2-PHBdT, O^4-PHBdT, and O^6-PHBdG in the four cell lines, where O^2-PHBdT and O^6-PHBdG displayed higher frequencies of formation than O^4-PHBdT. In the repair study, we carefully compared the levels of these lesions in NER-proficient and NER-deficient cells. Our results revealed that O^2-PHBdT and, to a lesser extent, O^4-PHBdT may serve as substrates for NER, whereas O^6-PHBdG cannot be repaired by NER. The different capacity of Chinese hamster ovary cells and human fibroblasts cells in repairing O^6-PHBdG suggests that AGT is responsible for the removal of this specific modification.[17,19,28,43] Thus, we interrogated how the accumulation of the three lesions in human cells is affected by co-exposure with an AGT inhibitor, O^6-benzylguanine. The results confirmed our hypothesis that AGT assumes an important role in the reversal of O^6-PHBdG and, to a lesser degree, O^4-PHBdT, which is in line with the notion that AGT recognizes major-groove lesions.[27,45]

It is worth comparing the results obtained for the pyridylhydroxybutylated lesions with those obtained previously for the pyridyloxobutylated lesions.[18] In this context, our previous study on O^2-POBdT, O^4-POBdT, and O^6-POBdG revealed that the formation of the three POB lesions is dose-dependent, and O^2-POBdT is most efficiently repaired by NER, O^4-POBdT

can be repaired at a lesser degree, whereas O^6-POBdG is not a substrate for NER.[18] The involvement of AGT in repairing O^6-PHBdG is in keeping with our previous observation of lower levels of O^6-POBdG in human skin fibroblasts than CHO cells.[18]

In summary, here we reported an LC-MS/MS method for the simultaneous measurement of three pyridylhydroxybutyl lesions, that is, O^2-PHBdT, O^4-PHBdT, and O^6-PHBdG, where O^4-PHBdT was, for the first time, found to be induced in mammalian cells upon exposure to pyridylhydroxybutylating agents. The method exhibited high sensitivity in quantification of targeted DNA lesions and its capacity to snapshot the levels of lesions in a repair study at different time intervals. The method may serve as a tool for investigating the involvement of DNA pyridylhydroxybutylation as a biomarker related to tobacco-induced cancer. In this regard, it will be important to examine, in the future, the occurrence and repair of these lesions in human lung cells and the lung tissues of smokers.

Supplementary Material

Refer to Web version on PubMed Central for supplementary material.

ACKNOWLEDGMENTS

This work was supported by the National Institute of Health (R01 ES025121), and N.P. was supported in part by an T32 Institutional Training Grant (ES018827).

REFERENCES

(1). Lindahl T, and Wood RD (1999) Quality control by DNA repair. Science 286, 1897–1905. [PubMed: 10583946]

(2). Fu D, Calvo JA, and Samson LD (2012) Balancing repair and tolerance of DNA damage caused by alkylating agents. Nat. Rev. Cancer 12, 104–120. [PubMed: 22237395]

(3). Shrivastav N, Li D, and Essigmann JM (2010) Chemical biology of mutagenesis and DNA repair: cellular responses to DNA alkylation. Carcinogenesis 31, 59–70. [PubMed: 19875697]

(4). Wynder EL, and Muscat JE (1995) The changing epidemiology of smoking and lung cancer histology. Environ. Health Perspect 103, 143–148.

(5). Hackshaw AK, Law MR, and Wald NJ (1997) The accumulated evidence on lung cancer and environmental tobacco smoke. BMJ 315, 980–988. [PubMed: 9365295]

(6). Nyberg F, and Pershagen G (1998) Passive smoking and lung cancer. Accumulated evidence on lung cancer and environmental tobacco smoke. BMJ [Br. Med. J.] 317, 347–348.

(7). Hoffmann D, and Hecht SS (1985) Nicotine-derived N-nitrosamines and tobacco-related cancer: current status and future directions. Cancer Res 45, 935–944. [PubMed: 3882226]

(8). Hecht SS, and Hoffmann D (1988) Tobacco-specific nitrosamines, an important group of carcinogens in tobacco and tobacco smoke. Carcinogenesis 9, 875–884. [PubMed: 3286030]

(9). Hecht SS (1998) Biochemistry, biology, and carcinogenicity of tobacco-specific N-nitrosamines. Chem. Res. Toxicol 11, 559–603. [PubMed: 9625726]

(10). Hecht SS (1999) Tobacco smoke carcinogens and lung cancer. J. Natl. Cancer Inst 91, 1194–1210. [PubMed: 10413421]

(11). Hecht SS (1999) DNA adduct formation from tobacco-specific N-nitrosamines. Mutat. Res., Fundam. Mol. Mech. Mutagen 424, 127–142.

(12). Hecht SS, Villalta PW, Sturla SJ, Cheng G, Yu N, Upadhyaya P, and Wang M (2004) Identification of O2-substituted pyrimidine adducts formed in reactions of 4-(acetoxymethylnitrosamino)- 1-(3-pyridyl)-1-butanone and 4-(acetoxymethylnitros- amino)-1-(3-pyridyl)-1-butanol with DNA. Chem. Res. Toxicol 17, 588–597. [PubMed: 15144215]

(13). Hecht SS, Stepanov I, and Carmella SG (2016) Exposure and metabolic activation biomarkers of carcinogenic tobacco-specific nitrosamines. Acc. Chem. Res 49, 106–114. [PubMed: 26678241]

(14). Peterson LA (2017) Context matters: contribution of specific DNA adducts to the genotoxic properties of the tobacco-specific nitrosamine NNK. Chem. Res. Toxicol 30, 420–433. [PubMed: 28092943]

(15). Stepanov I, and Hecht SS (2009) Mitochondrial DNA adducts in the lung and liver of F344 rats chronically treated with 4-(methylnitrosamino)-1-(3-pyridyl)-1-butanone and (S)-4-(methylnitrosamino)-1-(3-pyridyl)-1-butanol. Chem. Res. Toxicol 22, 406–414. [PubMed: 19166332]

(16). Balbo S, Johnson CS, Kovi RC, James-Yi SA, O'Sullivan MG, Wang M, Le CT, Khariwala SS, Upadhyaya P, and Hecht SS (2014) Carcinogenicity and DNA adduct formation of 4-(methylnitrosamino)-1-(3-pyridyl)-1-butanone and enantiomers of its metabolite 4-(methylnitrosamino)-1-(3-pyridyl)-1-butanol in F-344 rats. Carcinogenesis 35, 2798–2806. [PubMed: 25269804]

(17). Urban AM, Upadhyaya P, Cao Q, and Peterson LA (2012) Formation and repair of pyridyloxobutyl DNA adducts and their relationship to tumor yield in A/J mice. Chem. Res. Toxicol 25, 2167–2178. [PubMed: 22928598]

(18). Leng J, and Wang Y (2017) Liquid chromatography-tandem mass spectrometry for the quantification of tobacco-specific nitrosamine-induced DNA adducts in mammalian cells. Anal. Chem 89, 9124–9130. [PubMed: 28749651]

(19). Mijal RS, Thomson NM, Fleischer NL, Pauly GT, Moschel RC, Kanugula S, Fang Q, Pegg AE, and Peterson LA (2004) The repair of the tobacco specific nitrosamine derived adduct O6-[4-Oxo-4-(3-pyridyl)butyl]guanine by O6-alkylguanine-DNA alkyltransferase variants. Chem. Res. Toxicol 17, 424–434. [PubMed: 15025514]

(20). Carlson ES, Upadhyaya P, Villalta PW, Ma B, and Hecht SS (2018) Analysis and identification of 2'-deoxyadenosine-derived adducts in lung and liver DNA of F-344 rats treated with the tobacco-specific carcinogen 4-(Methylnitrosamino)-1-(3-pyridyl)-1-butanone and enantiomers of its metabolite 4-(Methylnitrosamino)-1-(3-pyridyl)-1-butanol. Chem. Res. Toxicol 31, 358–370. [PubMed: 29651838]

(21). Ma B, Zarth AT, Carlson ES, Villalta PW, Stepanov I, and Hecht SS (2017) Pyridylhydroxybutyl and pyridyloxobutyl DNA phosphate adduct formation in rats treated chronically with enantiomers of the tobacco-specific nitrosamine metabolite 4-(methylnitrosamino)-1-(3-pyridyl)-1-butanol. Mutagenesis 32, 561–570. [PubMed: 29186507]

(22). Lao Y, Villalta PW, Sturla SJ, Wang M, and Hecht SS (2006) Quantitation of pyridyloxobutyl DNA adducts of tobacco-specific nitrosamines in rat tissue DNA by high-performance liquid chromatography-electrospray ionization-tandem mass spectrometry. Chem. Res. Toxicol 19, 674–682. [PubMed: 16696570]

(23). Ma B, Villalta PW, Zarth AT, Kotandeniya D, Upadhyaya P, Stepanov I, and Hecht SS (2015) Comprehensive high-resolution mass spectrometric analysis of DNA phosphate adducts formed by the tobacco-specific lung carcinogen 4-(Methylnitrosamino)-1-(3-pyridyl)-1-butanone. Chem. Res. Toxicol 28, 2151–2159. [PubMed: 26398225]

(24). Du H, Leng J, Wang P, Li L, and Wang Y (2018) Impact of tobacco-specific nitrosamine-derived DNA adducts on the efficiency and fidelity of DNA replication in human cells. J. Biol. Chem 293, 11100–11108. [PubMed: 29789427]

(25). Ronai ZA, Gradia S, Peterson LA, and Hecht SS (1993) G to A transitions and G to T transversions in codon 12 of the Ki-ras oncogene isolated from mouse lung tumors induced by 4-(methylnitrosamino)-1-(3-pyridyl)-1-butanone (NNK) and related DNA methylating and pyridyloxobutylating agents. Carcinogenesis 14, 2419–2422. [PubMed: 7902220]

(26). Ma B, Zarth AT, Carlson ES, Villalta PW, Upadhyaya P, Stepanov I, and Hecht SS (2018) Methyl DNA phosphate adduct formation in rats treated chronically with 4-(Methylnitrosamino)-1-(3-pyridyl)-1-butanone and enantiomers of its metabolite 4-(Methylnitrosamino)-1-(3-pyridyl)-1-butanol. Chem. Res. Toxicol 31, 48–57. [PubMed: 29131934]

(27). Mishina Y, Duguid EM, and He C (2006) Direct reversal of DNA alkylation damage. Chem. Rev 106, 215–232. [PubMed: 16464003]

(28). Li L, Perdigao J, Pegg AE, Lao Y, Hecht SS, Lindgren BR, Reardon JT, Sancar A, Wattenberg EV, and Peterson LA (2009) The influence of repair pathways on the cytotoxicity and mutagenicity induced by the pyridyloxobutylation pathway of tobacco-specific nitrosamines. Chem. Res. Toxicol 22, 1464–1472. [PubMed: 19601657]

(29). Hecht SS (2012) Lung carcinogenesis by tobacco smoke. Int. J. Cancer 131, 2724–2732. [PubMed: 22945513]

(30). Peterson LA, and Hecht SS (2017) Tobacco, e-cigarettes, and child health. Curr. Opin. Pediatr 29, 225–230. [PubMed: 28059903]

(31). Choi JY, and Guengerich FP (2008) Kinetic analysis of translesion synthesis opposite bulky N^2- and O^6-alkylguanine DNA adducts by human DNA polymerase REV1. J. Biol. Chem 283, 23645–23655. [PubMed: 18591245]

(32). Weerasooriya S, Jasti VP, Bose A, Spratt TE, and Basu AK (2015) Roles of translesion synthesis DNA polymerases in the potent mutagenicity of tobacco-specific nitrosamine-derived O2-alkylthymidines in human cells. DNA Repair 35, 63–70. [PubMed: 26460881]

(33). Dator R, von Weymarn LB, Villalta PW, Hooyman CJ, Maertens LA, Upadhyaya P, Murphy SE, and Balbo S (2018) In vivo stable-isotope labeling and mass-spectrometry-based metabolic profiling of a potent tobacco-specific carcinogen in rats. Anal. Chem 90, 11863–11872. [PubMed: 30086646]

(34). Guo J, Yun BH, Upadhyaya P, Yao L, Krishnamachari S, Rosenquist TA, Grollman AP, and Turesky RJ (2016) Multiclass carcinogenic DNA adduct quantification in formalin-fixed paraffin-embedded tissues by ultraperformance liquid chromatography-tandem mass spectrometry. Anal. Chem 88, 4780–4787. [PubMed: 27043225]

(35). Monien BH, Schumacher F, Herrmann K, Glatt H, Turesky RJ, and Chesne C (2015) Simultaneous detection of multiple DNA adducts in human lung samples by isotope-dilution UPLC-MS/MS. Anal. Chem 87, 641–648. [PubMed: 25423194]

(36). Wang J, Yuan B, Guerrero C, Bahde R, Gupta S, and Wang Y (2011) Quantification of oxidative DNA lesions in tissues of Long-Evans Cinnamon rats by capillary high-performance liquid chromatography-tandem mass spectrometry coupled with stable isotope-dilution method. Anal. Chem 83, 2201–2209. [PubMed: 21323344]

(37). Xiao S, Guo J, Yun BH, Villalta PW, Krishna S, Tejpaul R, Murugan P, Weight CJ, and Turesky RJ (2016) Biomonitoring DNA adducts of cooked meat carcinogens in human prostate by nano liquid chromatography-high resolution tandem mass spectrometry: identification of 2-Amino-1-methyl-6-phenylimidazo[4,5-b]pyridine DNA adduct. Anal. Chem 88, 12508–12515. [PubMed: 28139123]

(38). Yu Y, Wang J, Wang P, and Wang Y (2016) Quantification of azaserine-induced carboxymethylated and methylated DNA lesions in cells by nanoflow liquid chromatography-nanoelectrospray ionization tandem mass spectrometry coupled with the stable isotope-dilution method. Anal. Chem 88, 8036–8042. [PubMed: 27441891]

(39). Sturla SJ, Scott J, Lao Y, Hecht SS, and Villalta PW (2005) Mass spectrometric analysis of relative levels of pyridyloxobutylation adducts formed in the reaction of DNA with a chemically activated form of the tobacco-specific carcinogen 4-(methylnitrosamino)-1-(3-pyridyl)-1-butanone. Chem. Res. Toxicol 18, 1048–1055. [PubMed: 15962940]

(40). Liu S, and Wang Y (2015) Mass spectrometry for the assessment of the occurrence and biological consequences of DNA adducts. Chem. Soc. Rev 44, 7829–7854. [PubMed: 26204249]

(41). Guo C, Xie C, Chen Q, Cao X, Guo M, Zheng S, and Wang Y (2018) A novel malic acid-enhanced method for the analysis of 5-methyl-2'-deoxycytidine, 5-hydroxymethyl-2'-deoxycytidine, 5-methylcytidine and 5-hydroxymethylcytidine in human urine using hydrophilic interaction liquid chromatography-tandem mass spectrometry. Anal. Chim. Acta 1034, 110–118. [PubMed: 30193624]

(42). Rolig RL, Layher SK, Santi B, Adair GM, Gu F, Rainbow AJ, and Nairn RS (1997) Survival, mutagenesis, and host cell reactivation in a Chinese hamster ovary cell ERCC1 knock-out mutant. Mutagenesis 12, 277–283. [PubMed: 9237774]

(43). Peterson LA, Liu XK, and Hecht SS (1993) Pyridyloxobutyl DNA adducts inhibit the repair of O^6-methylguanine. Cancer Res 53, 2780–2785. [PubMed: 8504419]

(44). Srivenugopal KS, Yuan XH, Friedman HS, and Ali-Osman F (1996) Ubiquitination-dependent proteolysis of O^6-methylguanine-DNA methyltransferase in human and murine tumor cells following inactivation with O6-benzylguanine or 1,3-bis(2-chloroethyl)-1-nitrosourea. Biochemistry 35, 1328–1334. [PubMed: 8573590]

(45). Mitra S (2007) MGMT: a personal perspective. DNA Repair 6 (8), 1064–1070. [PubMed: 17482889]

(46). Wang P, and Wang Y (2018) Cytotoxic and mutagenic properties of O6-alkyl-2'-deoxyguanosine lesions in Escherichia coli cells. J. Biol. Chem 293, 15033–15042. [PubMed: 30068548]

(47). Wang P, Amato NJ, Zhai Q, and Wang Y (2015) Cytotoxic and mutagenic properties of O^4-alkylthymidine lesions in Escherichia coli cells. Nucleic Acids Res 43, 10795–10803. [PubMed: 26400162]

(48). Zhai Q, Wang P, Cai Q, and Wang Y (2014) Syntheses and characterizations of the in vivo replicative bypass and mutagenic properties of the minor-groove O^2-alkylthymidine lesions. Nucleic Acids Res 42, 10529–10537. [PubMed: 25120272]

(49). Yu Y, Cui Y, Niedernhofer LJ, and Wang Y (2016) Occurrence, biological consequences, and human health relevance of oxidative stress-induced DNA damage. Chem. Res. Toxicol 29, 2008–2039. [PubMed: 27989142]

(50). Yu Y, Wang P, Cui Y, and Wang Y (2018) Chemical analysis of DNA damage. Anal. Chem 90, 556–576. [PubMed: 29084424]

(51). Vanden Bussche J, Moore SA, Pasmans F, Kuhnle GG, and Vanhaecke L (2012) An approach based on ultra-high pressure liquid chromatography-tandem mass spectrometry to quantify O6-methyl and O6-carboxymethylguanine DNA adducts in intestinal cell lines. J. Chromatogr. A 1257, 25–33. [PubMed: 22921361]

(52). Da Pieve C, Sahgal N, Moore SA, and Velasco-Garcia MN (2013) Development of a liquid chromatography/tandem mass spectrometry method to investigate the presence of biomarkers of DNA damage in urine related to red meat consumption and risk of colorectal cancer. Rapid Commun. Mass Spectrom 27, 2493–2503. [PubMed: 24097406]

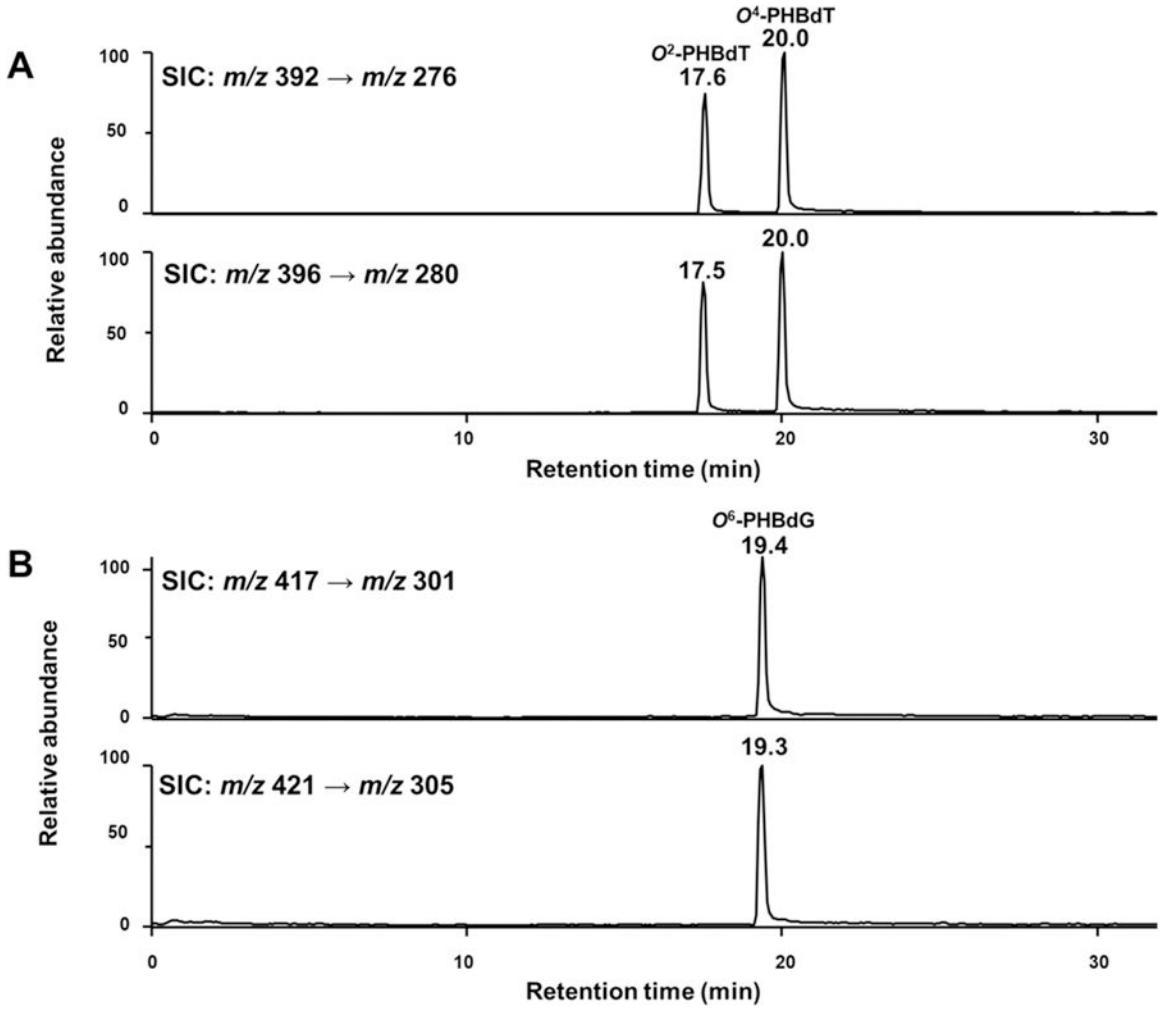

Figure 1.

Representative SICs for the *m*/*z* 392 → 276 (A, top panel), 396 → 280 (A, bottom panel), 417 → 301 (B, top panel), and 421 → 305 (B, bottom panel) transitions for the $[M + H]^+$ ions of the unlabeled and stable isotope (i.e., pyridine-d_4)-labeled O^2- and O^4-PHBdT (A) and O^6-PHBdG (B), respectively, in the enriched modified nucleoside mixture of genomic DNA extracted from the GM04429 cells treated with 10 μM NNALOAc for 24 h.

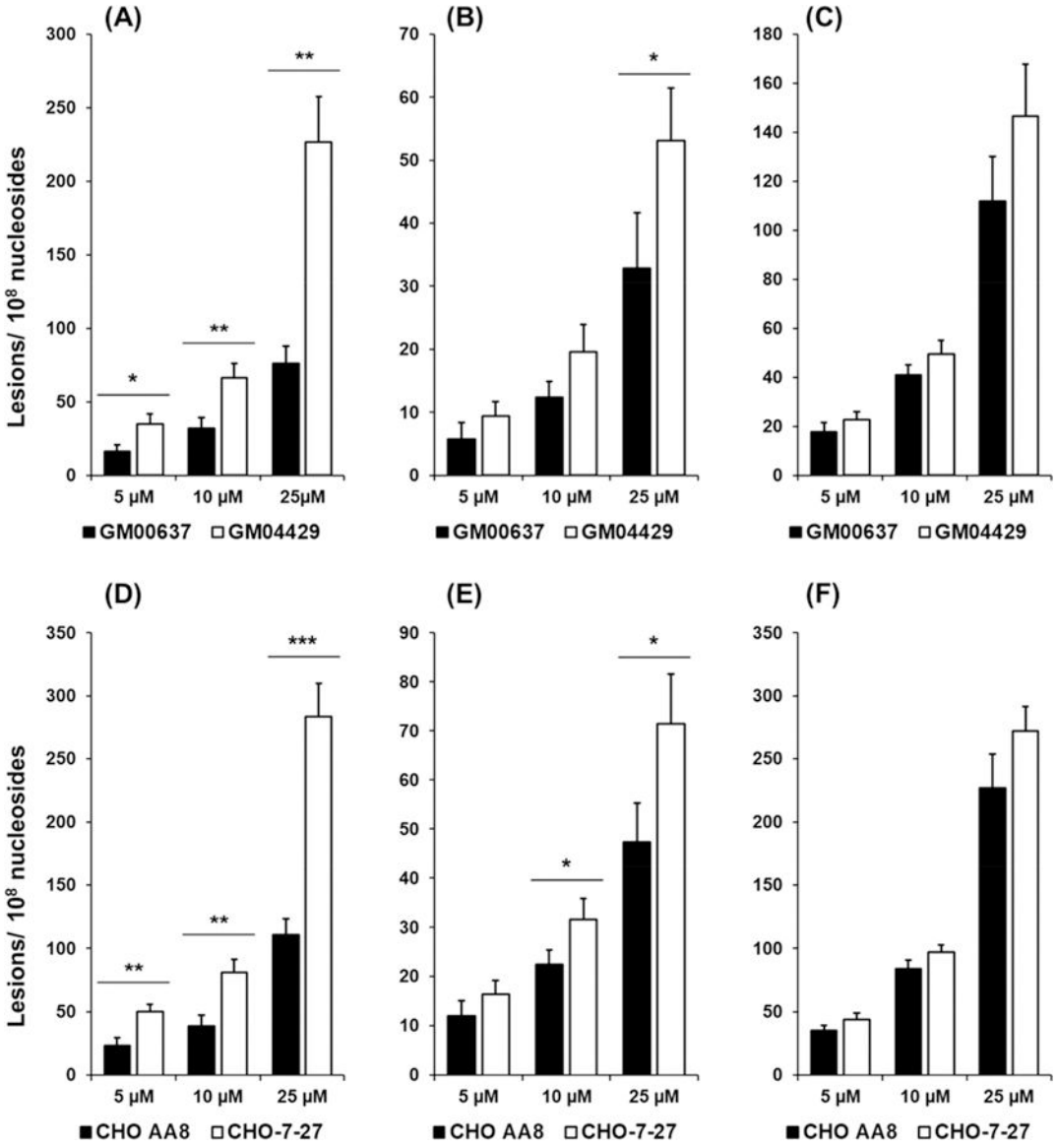

Figure 2.

Frequencies of O^2-PHBdT (A, D), O^4-PHBdT (B, E), and O^6-PHBdG (C, F) in DNA samples isolated from human skin fibroblast cells (A−C) that are repair proficient (GM00637) or deficient in XPA (GM04429) and Chinese hamster ovary cells (D−F) that are repair competent (CHO-AA8) or deficient in ERCC1 (CHO-7−27). The cells were exposed to the indicated concentrations of NNALOAc for 24 h. The data represent the mean and standard deviation of results obtained from three independent experiments. *, $0.01 \leqslant p < 0.05$; **, $0.001 \leqslant p < 0.01$; ***, $p < 0.001$. The p values were calculated by using unpaired two-tailed student's t-test.

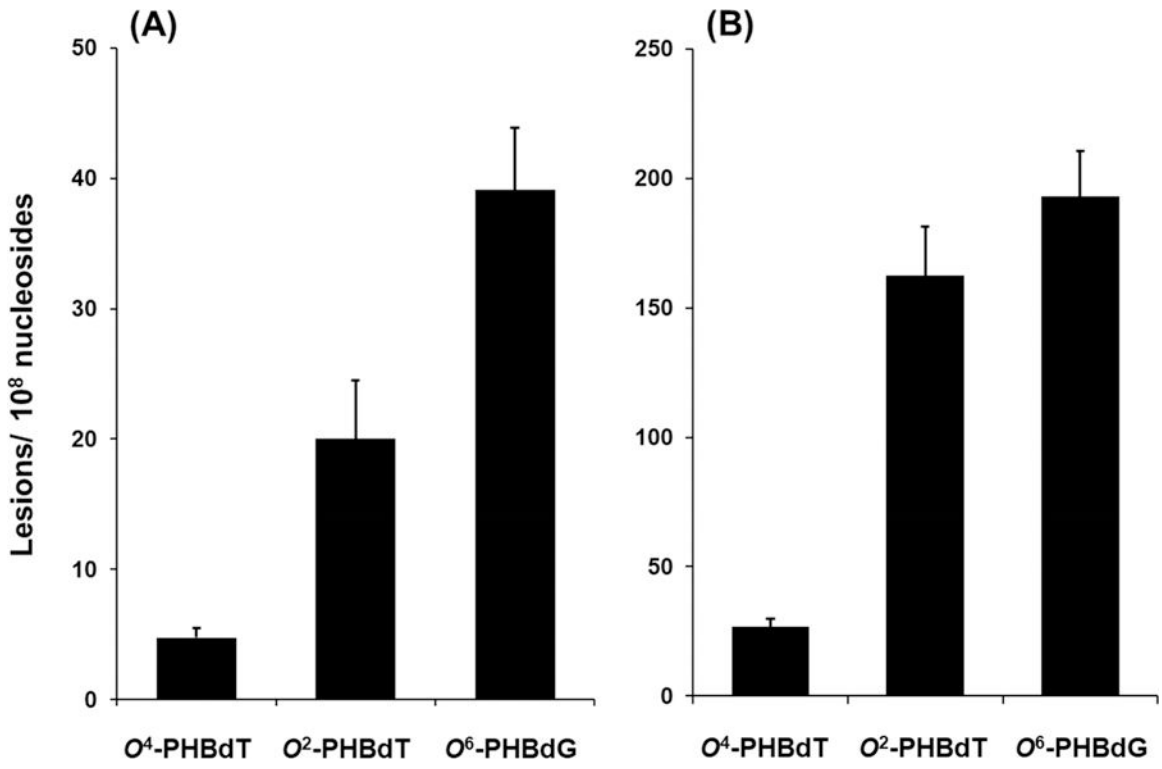

Figure 3.

Frequencies of O^4-PHBdT, O^2-PHBdT, and O^6-PHBdG in calf thymus DNA treated with (A) 10 μg (37.4 μM) and (B) 50 μg (187 μM) NNALOAc in the presence of porcine liver esterase.

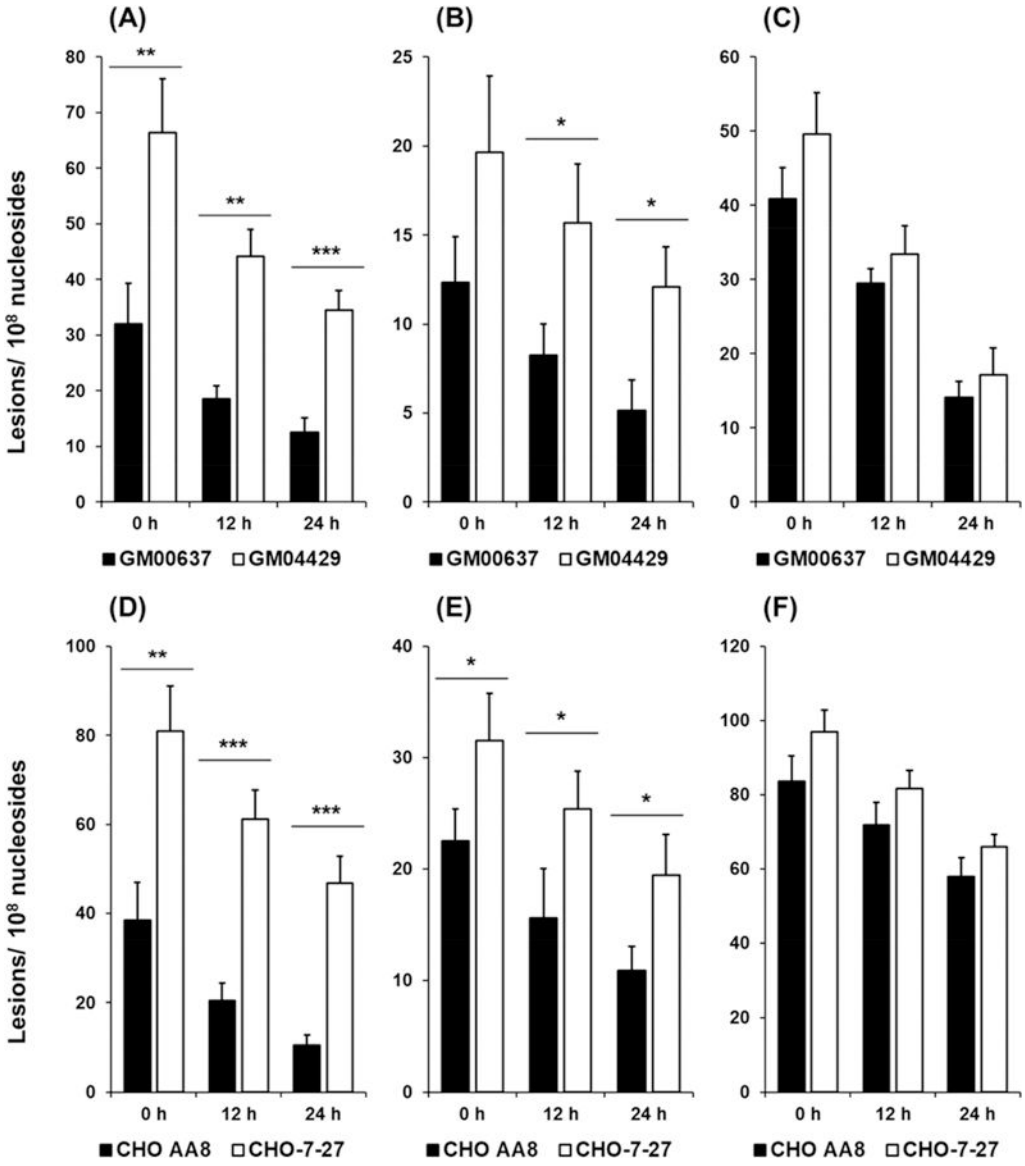

Figure 4.

LC-MS/MS for monitoring the repair of O^2-PHBdT (A, D), O^4-PHBdT (B, E), and O^6-PHBdG (C, F) in human skin fibroblast (A−C) and Chinese hamster ovary (D−F) cells. After a 24 h exposure to 10 μM NNALOAc, the media was exchanged, and the cells were harvested immediately or 12 or 24 h later. The data represent the mean and standard deviation of results obtained from three independent experiments. *, $0.01 \leqslant p < 0.05$; **, $0.001 \leqslant p < 0.01$; ***, $p < 0.001$. The p values were calculated by using unpaired two-tailed Student's t-test.

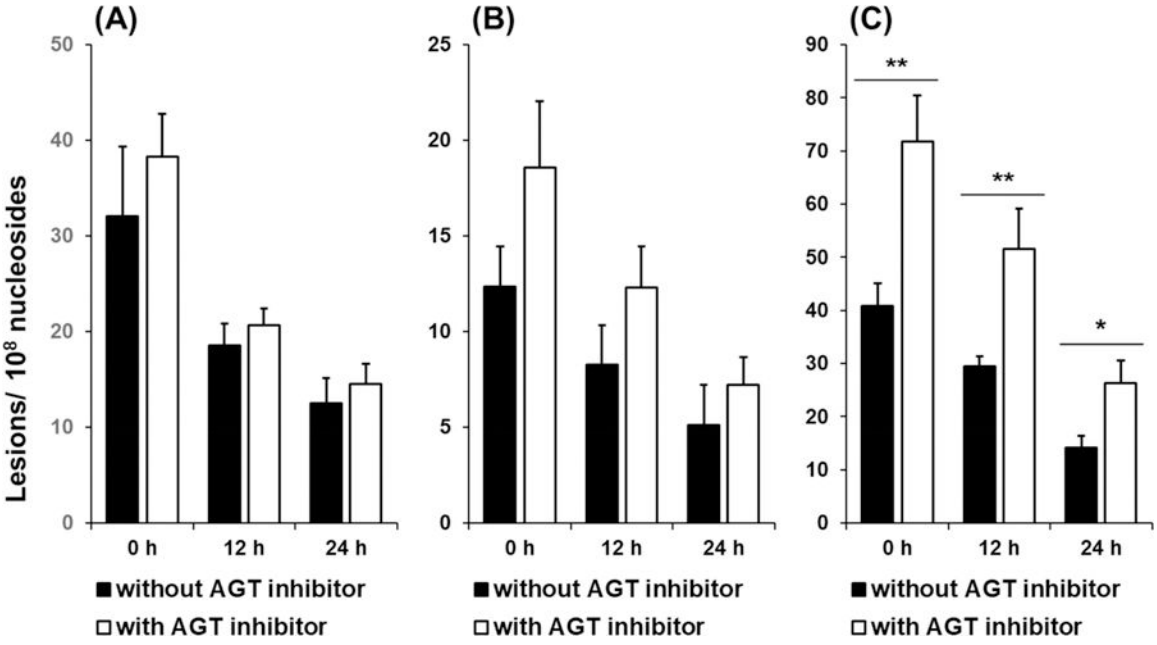

Figure 5.

Repair of O^2-PHBdT (A), O^4-PHBdT (B), and O^6-PHBdG (C) in GM00637 human skin fibroblast cells following a 24 h exposure to 10 μM NNALOAc alone or concurrently with 20 μM O^6-benzylguanine (to deplete AGT). The data represent the mean and standard deviation of results obtained from three independent experiments. *, $0.01 \leqslant p < 0.05$; **, $p < 0.01$. The p values were calculated by using unpaired two-tailed Student's t-test.

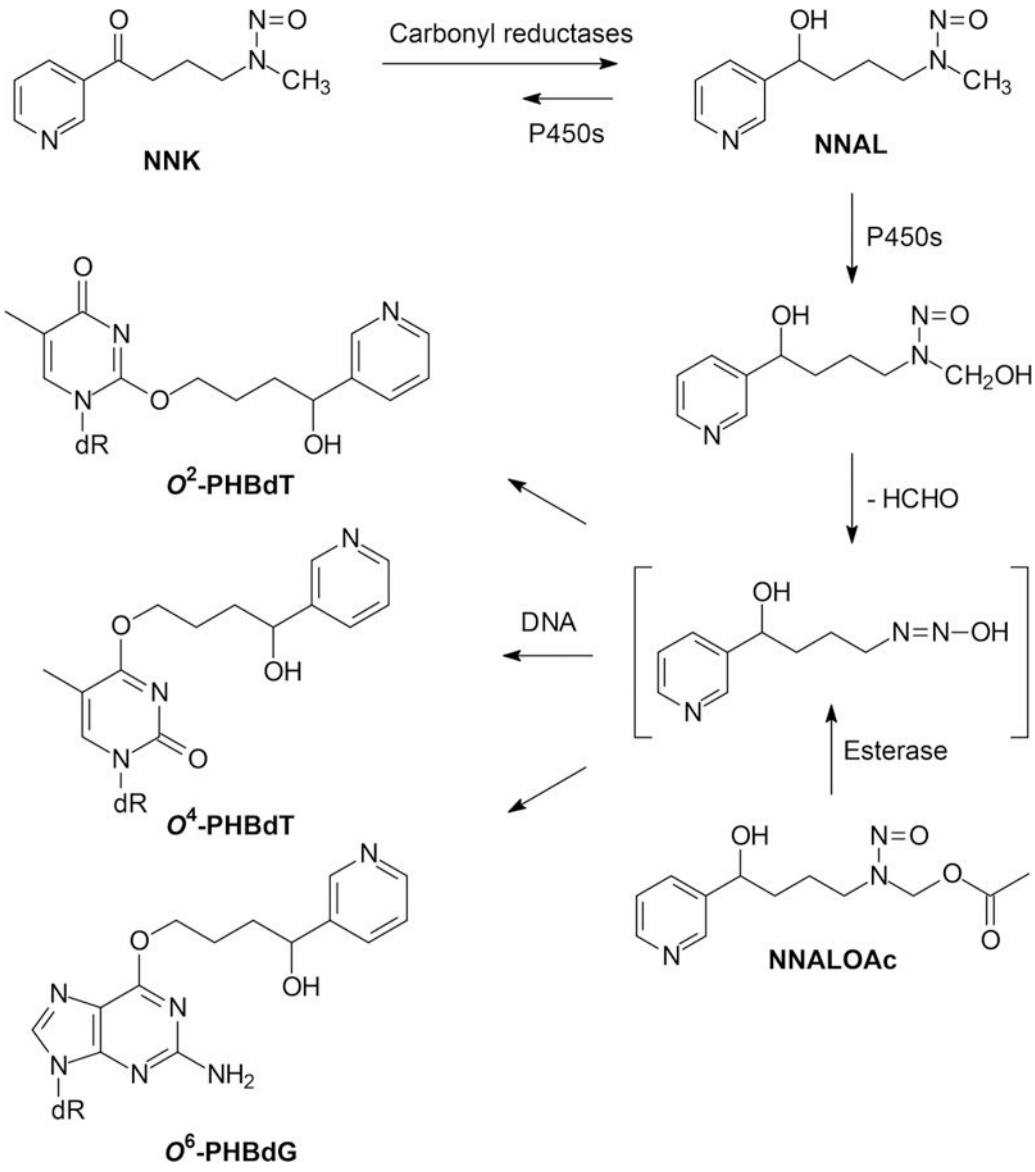

Scheme 1.

Activation of NNALOAc by Cellular Esterases, and Metabolic Activation of NNK and NNAL by Cytochrome P450 Enzymes, Followed by the Conjugation of the Resulting Common Reactive Intermediate with DNA to Yield O^2-PHBdT, O^4-PHBdT, and O^6-PHBdG[a]

Table 1.

Intraday and Interday Evaluation on Precision and Accuracy, as Represented by Relative Standard Deviation (RSD) and Recovery, Respectively, for the Measurements of O^2-PHBdT, O^4-PHBdT, and O^6-PHBdG

ODN amount (fmol)	expected lesion frequency in 10 μg DNA (/10^8 nucleosides)	Intraday		interday	
		RSD (%)	recovery (%)	RSD (%)	recovery (%)
O^2-PHBdT					
5.0	15.4	8.1	91.2	14.9	84.9
15	46.2	5.6	89.3	9.1	90.0
50	154.0	7.4	90.5	11.6	87.1
O^4-PHBdT					
5.0	15.4	9.2	93.4	11.0	90.4
15	46.2	7.7	88.2	13.9	89.5
50	154.0	10.1	92.5	10.7	87.8
O^6-PHBdG					
5.0	15.4	7.8	95.2	9.5	89.6
15	46.2	6.1	94.6	14.3	97.1
50	154.0	3.8	90.7	11.5	91.0